

## ARTICLE

Infrared Spectroscopy of CO<sub>2</sub> Transformation by Group III Metal Monoxide Cations<sup>†</sup>

Dong Yang<sup>a,b,†</sup>, Ming-zhi Su<sup>a,b,†</sup>, Hui-jun Zheng<sup>a,b</sup>, Zhi Zhao<sup>a</sup>, Xiang-tao Kong<sup>a</sup>, Gang Li<sup>a</sup>, Hua Xie<sup>a</sup>, Wei-qing Zhang<sup>a</sup>, Hong-jun Fan<sup>a\*</sup>, Ling Jiang<sup>a\*</sup>

*a. State Key Laboratory of Molecular Reaction Dynamics, Collaborative Innovation Center of Chemistry for Energy and Materials, Dalian Institute of Chemical Physics, Chinese Academy of Sciences, Dalian 116023, China*

*b. University of Chinese Academy of Sciences, Beijing 100049, China*

(Dated: Received on October 6, 2019; Accepted on October 12, 2019)

Infrared photodissociation spectroscopy of mass-selected [MO(CO<sub>2</sub>)<sub>n</sub>]<sup>+</sup> (M=Sc, Y, La) complexes indicates that the conversion from the solvated structure into carbonate one can be achieved by the ScO<sup>+</sup> cation at *n*=5 and by the YO<sup>+</sup> cation at *n*=4, while only the solvated structures are observed for the LaO<sup>+</sup> cation. These findings suggest that both the ScO<sup>+</sup> and YO<sup>+</sup> cations are able to fix CO<sub>2</sub> into carbonate. Quantum chemical calculations are performed on [MO(CO<sub>2</sub>)<sub>n</sub>]<sup>+</sup> to identify the structures of the low-lying isomers and to assign the observed spectral features. Theoretical analyses show that the [YO(CO<sub>2</sub>)<sub>n</sub>]<sup>+</sup> complex has the smallest barrier for the conversion from the solvated structure into carbonate one, while [LaO(CO<sub>2</sub>)<sub>n</sub>]<sup>+</sup> exhibits the largest conversion barrier among the three metal oxide cations. The present system affords a model in clarifying the effect of different metals in catalytic CO<sub>2</sub> transformation at the molecular level.

**Key words:** Infrared spectroscopy, CO<sub>2</sub> transformation, Metal monoxide cation

## I. INTRODUCTION

The chemical conversion and fixation of carbon dioxide is one of the most extensively studied catalytic reactions because of their great environmental significance in global warming mitigation and various promising applications in synthetic and material chemistry [1–3]. Metal compounds play an important role in the catalytic transformation of CO<sub>2</sub> [4, 5]. Gas-phase optical spectroscopy of mass-selected clusters has provided great insights into the single-site catalysis processes at the molecular level [6–10].

The monodentate coordination M( $\eta^1$ -CO<sub>2</sub>), bidentate coordination M( $\eta^2$ -CO<sub>2</sub>), or inserted OMCO structures have been observed in the neutral metal-CO<sub>2</sub> complexes [6, 11, 12]. In general, the weakly-bound M<sup>+</sup>-OCO structure is dominated in the interaction of CO<sub>2</sub> with a metal cation [7, 13–23]. Interestingly, the metal oxide-carbonyls [OMCO(CO<sub>2</sub>)<sub>*n*-1</sub>]<sup>+</sup> (M=Ti, Ni, Si) present in the *n*≥5 clusters [16–18] and a bent CO<sub>2</sub><sup>-</sup> fashion appears in [V(CO<sub>2</sub>)<sub>*n*</sub>]<sup>+</sup> (*n*≥7) [20, 24]. In the [M(CO<sub>2</sub>)<sub>*n*</sub>]<sup>-</sup> cluster anions, the activation of CO<sub>2</sub> is

very effectively achieved by the excess electron of the metal anion [8, 10, 25–35]. While the bidentate [M( $\eta^2$ -CO<sub>2</sub>)]<sup>-</sup> configuration is preferred for the first-row transition metal anions, the metalloformate [M( $\eta^1$ -CO<sub>2</sub>)]<sup>-</sup> structure is favored for the Bi<sup>-</sup>, Cu<sup>-</sup>, Ag<sup>-</sup>, and Au<sup>-</sup> anions [25, 26, 28, 30]. An oxalate motif has ever been captured in the [Bi(CO<sub>2</sub>)<sub>*n*</sub>]<sup>-</sup> (*n*≥5) clusters [30]. Notable CO<sub>2</sub> activation is accessed in a Ni(I) compound [36] and a [ClMg( $\eta^2$ -O<sub>2</sub>C)]<sup>-</sup> complex [37].

Recent studies have shown that group III metal oxides are promising candidates for catalytic applications [2, 38, 39]. The reaction of YO<sup>+</sup> with CO<sub>2</sub> was studied using ion beam mass spectrometry and its bond dissociation energy was measured to be (0.89±0.05) eV by collisional activation experiments with Xe [40]. Collision-induced dissociation experiments indicated that the [YO(CO<sub>2</sub>)<sub>*n*</sub>]<sup>+</sup> complex consists of a weakly-bound structure [40]. Infrared photodissociation (IRPD) spectroscopic studies of [YO(CO<sub>2</sub>)<sub>*n*</sub>]<sup>+</sup> reveal that the first three CO<sub>2</sub> molecules are weakly bound to YO<sup>+</sup> and a carbonate motif is formed in the *n*≥4 clusters, which occurs via a solvation-induced electron transfer from the ligands to metal [41]. IRPD spectra of the [NbO<sub>2</sub>(CO<sub>2</sub>)<sub>*n*</sub>]<sup>+</sup> and [TaO<sub>2</sub>(CO<sub>2</sub>)<sub>*n*</sub>]<sup>+</sup> cluster cations show the dominant solvated structures, with some characteristic features of a possible carbonate moiety in the *n*≥4 clusters [42]. In the [TiO(CO<sub>2</sub>)<sub>*n*</sub>]<sup>-</sup> cluster anions, the formation of carbonate, oxalato, oxo,  $\eta^2$ -(O,O), and carbonyl ligands was identified [35]. Matrix-isolation IR spectroscopy of

<sup>†</sup>The special topic on “The 35th International Symposium on Free Radical (ISFR 2019)”.

<sup>†</sup>These authors contributed equally to this work.

\* Authors to whom correspondence should be addressed. E-mail: ljiang@dicp.ac.cn, fanhj@dicp.ac.cn

the neutral ScO with CO<sub>2</sub> has characterized a carbonate ScCO<sub>3</sub> complex [43]. Herein, we report an IR study on the interaction of CO<sub>2</sub> with the ScO<sup>+</sup> and LaO<sup>+</sup> cations using the IRPD spectroscopy and quantum chemical calculations. Combined with the preliminary study of the [YO(CO<sub>2</sub>)<sub>n</sub>]<sup>+</sup> system [41], the systematic experimental results show that CO<sub>2</sub> can be converted into carbonate by the ScO<sup>+</sup> and YO<sup>+</sup> cations instead of LaO<sup>+</sup>, which is supported by theoretical calculations.

## II. EXPERIMENTS

IR spectra of the [MO(CO<sub>2</sub>)<sub>n</sub>]<sup>+</sup> (M=Sc and La) clusters are measured using an IRPD apparatus, which has been previously described in detail [41, 44]. The [MO(CO<sub>2</sub>)<sub>n</sub>]<sup>+</sup> complexes are prepared by a pulsed laser vaporization source with supersonic expansion of 2% O<sub>2</sub> seeded in CO<sub>2</sub>. The cluster cations of interest are mass-selected and decelerated into the extraction region of a time-of-flight (TOF) mass spectrometer. Here, they interact with a single pass of the IR laser from a Laservision OPO/OPA IR laser. The photodissociation fragments and parent cations are analyzed using the TOF mass spectrometer. Typical spectra are recorded by scanning the infrared laser in step of 2 cm<sup>-1</sup>. The IRPD spectra are acquired by monitoring the fragment ions as a function of the wavelength of tunable infrared laser.

## III. THEORETICAL METHOD

Electronic structure calculations are carried out using the Gaussian 09 program [45]. Recent study of the [YO(CO<sub>2</sub>)<sub>n</sub>]<sup>+</sup> complexes has shown that the B3LYP functional augmented with a dispersion correction (B3LYP-D) is able to reproduce the experimental IR spectroscopic observations [41]. Therefore, this functional is utilized for the present calculations as well. The DZP basis set is used for the carbon, oxygen, nitrogen, and hydrogen atoms, and the LanL2DZ ECP basis set for the scandium, yttrium, and lanthanum atoms. Tight convergence of the optimization and the self-consistent field procedures is imposed, and an ultra-fine grid is used. To obtain relative energies and conversion barriers, the single point calculations are carried out at the B2PLYP(full)/def2-TZVP level based on the B3LYP-D/DZP-LanL2DZ optimized structures. The calculated IR spectra are derived from the B3LYP-D scaled harmonic frequencies (scaling factor: 0.964) [41] and are convoluted using a Gaussian line shape function with a 5 cm<sup>-1</sup> full width at half-maximum (FWHM).

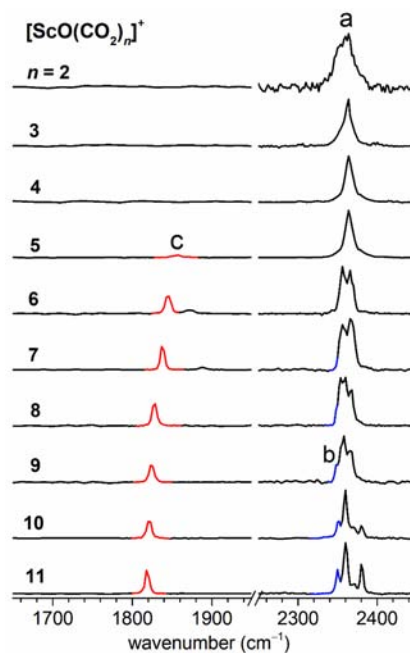


FIG. 1 Experimental IRPD spectra of the [ScO(CO<sub>2</sub>)<sub>n</sub>]<sup>+</sup> ( $n=2-11$ ) complexes.

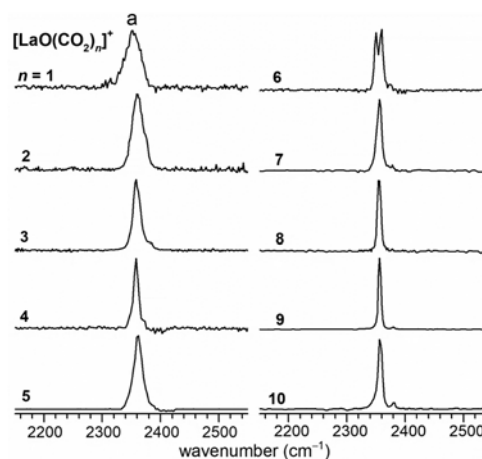


FIG. 2 Experimental IRPD spectra of the [LaO(CO<sub>2</sub>)<sub>n</sub>]<sup>+</sup> ( $n=1-10$ ) complexes.

## IV. RESULTS AND DISCUSSION

The time-of-flight mass spectra of the products generated by a pulsed laser vaporization of scandium and lanthanum targets under the supersonic expansion are shown in FIG. S1 and FIG. S2 in supplementary materials, respectively. The metal monoxide-CO<sub>2</sub> cationic complexes in the form of [MO(CO<sub>2</sub>)<sub>n</sub>]<sup>+</sup> (M=Sc and La,  $n=1-15$ ) are dominated in the mass spectral signals. Additional signals are assigned to the [M<sub>2</sub>O<sub>2</sub>(CO<sub>2</sub>)<sub>n</sub>]<sup>+</sup> species with relatively weak intensities as compared to [MO(CO<sub>2</sub>)<sub>n</sub>]<sup>+</sup>.

FIG. 1 and FIG. 2 show the experimental IR spec-

TABLE I Experimental band positions (in  $\text{cm}^{-1}$ ), calculated scaled harmonic vibrational frequencies of the lowest-lying isomers for  $[\text{ScO}(\text{CO}_2)_n]^+$  ( $n=2-11$ ).

$n$	Band a		Band b		Band c	
	Expt.	Calc.	Expt.	Calc.	Expt.	Calc.
2	2364	2370				
3	2364	2366				
4	2364	2365				
5	2364	2366			1858	1833
6	2356	2352			1846	1828
	2366	2365				
7	2356	2353	2348	2347	1837	1811
	2366	2360	2348	2347		
8	2354	2354	2348	2350	1829	1798
	2360	2359				
	2368	2363				
9	2358		2348		1823	
	2366		2348		1823	
10	2360		2352		1820	
	2380					
11	2360		2350		1818	
	2380		2350		1818	

Band a: antisymmetric stretch of  $\text{CO}_2$  in the first solvation shell, band b: antisymmetric stretch of  $\text{CO}_2$  in the second solvation shell, band c: C–O stretch of  $\text{CO}_3^{2-}$ .

tra of  $[\text{ScO}(\text{CO}_2)_n]^+$  ( $n=2-11$ ) and  $[\text{LaO}(\text{CO}_2)_n]^+$  ( $n=1-10$ ), respectively. The only fragmentation pathways observed involve loss of  $\text{CO}_2$ . The nearly linear laser power dependence of the fragmentation signal is confirmed and the IR spectra are normalized according to the IR power. Band positions of  $[\text{MO}(\text{CO}_2)_n]^+$  ( $\text{M}=\text{Sc}$  and  $\text{La}$ ) are listed in Tables I and II, respectively.

In the experimental IR spectra of  $[\text{ScO}(\text{CO}_2)_n]^+$  (FIG. 1), three main features are observed, labeled a–c. Band a is centered around  $2364 \text{ cm}^{-1}$ , which is characteristic of the antisymmetric stretch of  $\text{CO}_2$  in the first coordination sphere [7, 8, 10, 13–18, 20–23, 41, 42]. Band b is observed around  $2348 \text{ cm}^{-1}$ , which appears as a small shoulder at  $n=7$  and the intensity is increased in the large clusters. This band position is characteristic of the antisymmetric stretching vibration of free  $\text{CO}_2$  ( $2349 \text{ cm}^{-1}$ ) [7, 8, 10, 20]. Band c is weakly observed at the  $n=5$  cluster and red-shifts from  $1858 \text{ cm}^{-1}$  to  $1818 \text{ cm}^{-1}$  between  $[\text{ScO}(\text{CO}_2)_5]^+$  and  $[\text{ScO}(\text{CO}_2)_{11}]^+$ , which is similar to the  $[\text{YO}(\text{CO}_2)_n]^+$  ( $n=4-11$ ) with the characteristics of the C–O stretch [41]. In contrast, only one main feature centered around  $2360 \text{ cm}^{-1}$  (labeled a) appears in the IR spectra of  $[\text{LaO}(\text{CO}_2)_n]^+$  ( $n=1-10$ ) (FIG. 2), while no obvious band is observed in the  $1000-2200 \text{ cm}^{-1}$  region.

To identify the minimum-energy structures and to

TABLE II Experimental band positions (in  $\text{cm}^{-1}$ ), calculated scaled harmonic vibrational frequencies of the most-likely isomers for  $[\text{LaO}(\text{CO}_2)_n]^+$  ( $n=1-10$ ).

$n$	Band a	
	Expt.	Calc.
1	2352	2369
2	2360	2366
3	2358	2362
4	2358	2362
5	2362	2366
6	2350, 2360, 2375	2351, 2364, 2378
7	2356, 2378	2360, 2380
8	2356, 2380	
9	2356, 2380	
10	2356, 2380	

Band a: antisymmetric stretch of  $\text{CO}_2$  in the first solvation shell

understand the experimental spectral features, quantum chemical calculations are carried out using the B3LYP-D functional. Optimized structures of the two kinds of isomers for  $[\text{MO}(\text{CO}_2)_n]^+$  ( $\text{M}=\text{Sc}$  and  $\text{La}$ ) are shown in FIG. 3. The calculated IR spectra of  $[\text{ScO}(\text{CO}_2)_n]^+$  ( $n=2-8$ ) are depicted in FIG. 4 and those of  $[\text{LaO}(\text{CO}_2)_n]^+$  ( $n=1-8$ ) are shown in FIG. S3 (supplementary materials), respectively. The calculated band positions of  $[\text{ScO}(\text{CO}_2)_n]^+$  and  $[\text{LaO}(\text{CO}_2)_n]^+$  are given in Tables I and II, respectively.

Two binding motifs of solvated and carbonate structures are obtained, which are similar to those reported recently for the  $[\text{YO}(\text{CO}_2)_n]^+$  system [41]. For  $[\text{ScO}(\text{CO}_2)_n]^+$ , the solvated structures, labeled  $n\text{S}$  in FIG. 3, are predicted to be the lowest in energy for the  $n=1-4$  clusters; the most stable isomer of the  $n=5$  cluster consists of a carbonate binding motif (labeled  $n\text{C}$ ), which retains all of the lowest-energy isomers of the larger clusters. Similar features of minimum-energy structures are obtained for the  $[\text{LaO}(\text{CO}_2)_n]^+$  clusters (FIG. 3). Slight structural difference is found in  $[\text{ScO}(\text{CO}_2)_5]^+$  where one  $\text{CO}_2$  ligand is coordinated opposite to the carbonate or the oxygen on the axis. In contrast, all the four  $\text{CO}_2$  ligands are bound to the metal in the equatorial plane in  $[\text{LaO}(\text{CO}_2)_5]^+$ .

For the  $[\text{ScO}(\text{CO}_2)_n]^+$  ( $n=2-8$ ) clusters, the agreement of the experimental IR spectra with the calculated ones (FIG. 1 and FIG. 4), in particular with the relative band positions and the size-dependent trends, is observed, supporting our initial assignments of these bands. The antisymmetric stretching vibrational frequencies of  $\text{CO}_2$  in the first solvation shell of the most stable isomers are predicted to be centered around  $2360 \text{ cm}^{-1}$  (Table I), which are consistent with the experimental values of band a. In the  $[\text{ScO}(\text{CO}_2)_7]^+$  cluster, an antisymmetric stretch of  $\text{CO}_2$  in the second sol-

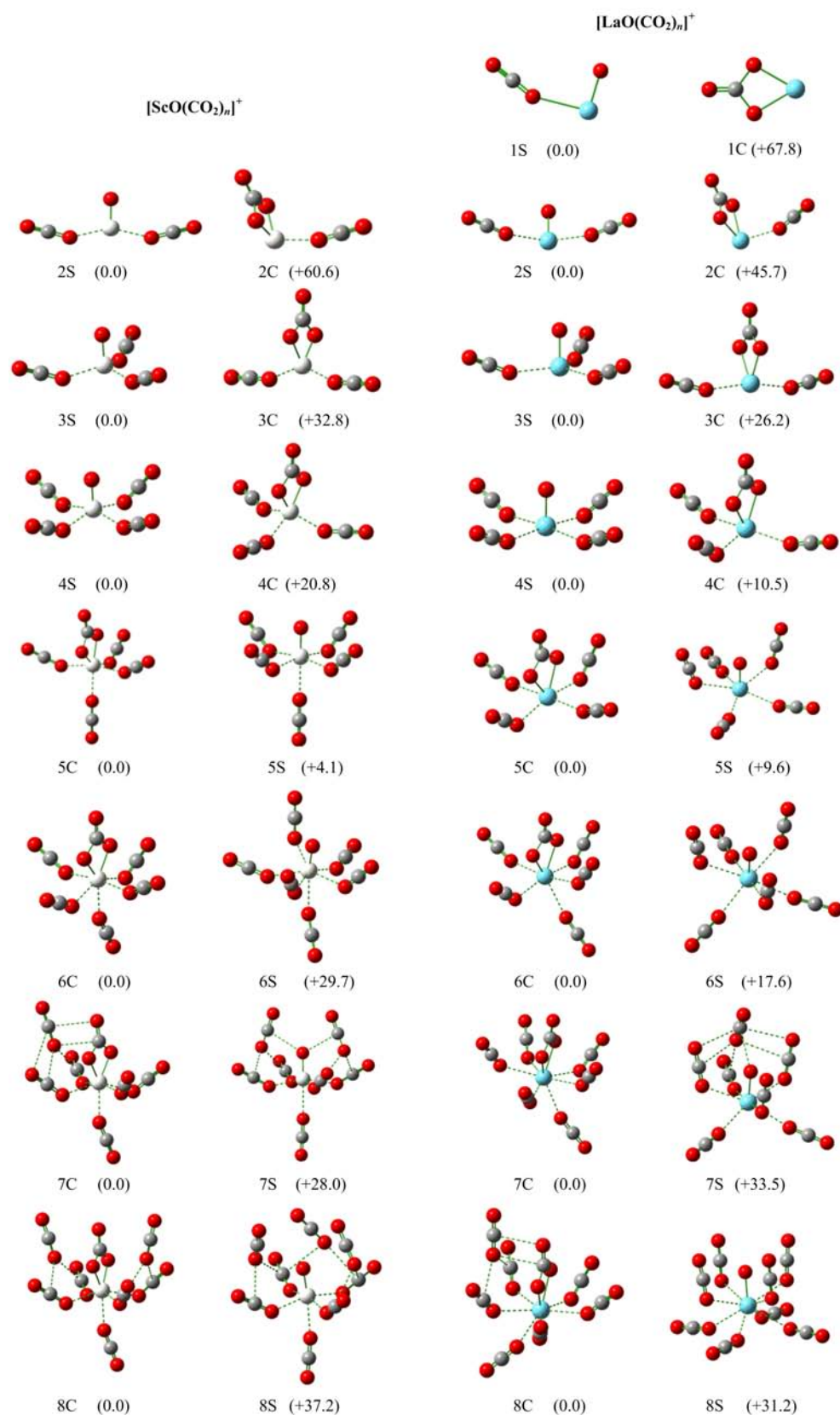


FIG. 3 Representatively optimized structures of the [ScO(CO<sub>2</sub>)<sub>n</sub>]<sup>+</sup> ( $n=2-8$ ) and [LaO(CO<sub>2</sub>)<sub>n</sub>]<sup>+</sup> ( $n=1-8$ ) complexes (Sc: white, La: cyan, C: gray, O: red). Relative energies are given in kJ/mol.

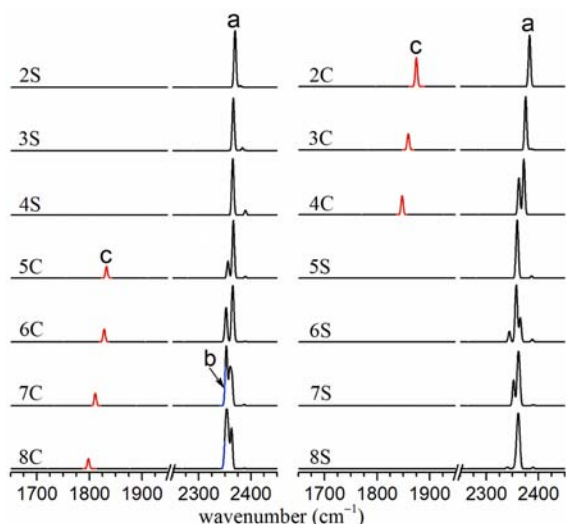


FIG. 4 Calculated IR spectra of the solvated and carbonate isomers for  $[\text{ScO}(\text{CO}_2)_n]^+$  ( $n=2-8$ ).

vation shell is calculated to be  $2347\text{ cm}^{-1}$ , which also appears in the simulated IR spectra of the  $n=8$  cluster, reproducing the experimental band b. In the calculated IR spectrum of the most stable structure for  $[\text{ScO}(\text{CO}_2)_5]^+$  (5C), the band at  $1833\text{ cm}^{-1}$  is due to the C–O stretch of carbonate core, which is consistent with the experimental value of band c ( $1858\text{ cm}^{-1}$ ) (Table I and FIGs. 1 and 4). The calculated frequency of band c red-shifts from  $1833\text{ cm}^{-1}$  to  $1798\text{ cm}^{-1}$  in-between the  $n=5$  and  $n=8$  clusters, which is in accord with the size-dependent trend observed in the experimental IR spectra.

For the  $[\text{LaO}(\text{CO}_2)_n]^+$  ( $n=1-8$ ) clusters, the calculated IR spectra of solvated structures (FIG. S3 in supplementary materials) are consistent with the experimental spectra (FIG. 2). In the calculated IR spectra of carbonate structures, the predicted C–O stretches of carbonate core are absent in the experimental spectra. It thus appears that the experimental spectra of  $[\text{LaO}(\text{CO}_2)_n]^+$  ( $n=1-10$ ) show the evidence of the formation of solvated structures, with the absence of carbonate structures.

The conversion barrier from the solvated structure into carbonate one of  $[\text{MO}(\text{CO}_2)_5]^+$  calculated at the B2PLYP/def2-TZVP level for Sc, Y, and La is 28.9, 14.4, and 32.2 kJ/mol (FIG. 5), respectively. This indicates that the  $[\text{YO}(\text{CO}_2)_5]^+$  complex has the smallest barrier for the conversion from the solvated structure into carbonate one, while  $[\text{ScO}(\text{CO}_2)_5]^+$  exhibits a slightly larger conversion barrier, supporting the experimental observation of coordination-induced  $\text{CO}_2$  fixation into carbonate by the  $\text{ScO}^+$  and  $\text{YO}^+$  cations. Note that the conversion barrier for the  $\text{LaO}^+(\text{CO}_2)_n$  system is not significantly larger than that for  $\text{ScO}^+$  and  $\text{YO}^+$ , an alternative reason for the absence of carbonate formation in the  $\text{LaO}^+(\text{CO}_2)_n$  system could

be that the conversion rate of solvated  $[\text{LaO}(\text{CO}_2)_n]^+$  complex to carbonate  $[\text{La}(\text{CO}_3)(\text{CO}_2)_{n-1}]^+$  species is much slower than that of  $[\text{ScO}(\text{CO}_2)_n]^+$  complex to carbonate  $[\text{Sc}(\text{CO}_3)(\text{CO}_2)_{n-1}]^+$  species. Recent gas-phase IRPD spectroscopy of the  $[\text{Pt}_4\text{CO}_2]^-$  cluster identified a molecularly-adsorbed isomer instead of a fully-dissociated structure (the global minimum) [33]. Similarly, higher-energy isomers on the potential energy surface have also been observed in several cluster systems [46, 47].

As analyzed for the  $[\text{YO}(\text{CO}_2)_n]^+$  system [41], the conversion of  $\text{M}=\text{O}$  and  $\text{CO}_2$  undergoes a 2+2 cycloaddition transition state, and the negative charge on O is beneficial for its nucleophilic attacking to C center of  $\text{CO}_2$  ligand. The  $\text{CO}_2$  conversion from the solvated structure into carbonate one is assisted by donating electrons from the ligands to the metal. The conversion barrier decreases with the increase of cluster size. The Mulliken charges of metal and O atoms of the MO unit in the  $[\text{MO}(\text{CO}_2)_n]^+$  solvated structures are given in Table S1 (supplementary materials). It can be seen from Table S1 that the difference in the Mulliken charge of metal atom is more prominent than that of O atom. The Sc and Y atoms are more electron rich than the La atom, suggesting a more favorable  $\text{CO}_2$  carbonation, which is consistent with the present experimental observations.

Previous computational studies on the conversion of  $[\text{YO}(\text{CO}_2)_n]^+$  to  $[\text{Y}(\text{CO}_3)_n]^+$  ( $\text{L}=\text{H}_2\text{O}$ ,  $\text{NH}_3$ , and  $\text{NHC}$  ( $N,N'$ -bis(methyl)imidazol-2-ylidene)) indicated that the carbonation would become easier via the increase of the donating power of the ligand [41]. Further experimental investigation of  $\text{CO}_2$  transformation in the ligand-doped  $[\text{MO}(\text{CO}_2)_n]^+$  systems is in progress. These studies would shed insights into molecular-level understanding of different degrees of activation of small molecules by tuning metals, ligands, cluster sizes, and supplementary materials.

## V. CONCLUSION

Gas-phase vibrational spectroscopic and theoretical studies on the reaction of  $\text{CO}_2$  with the  $\text{ScO}^+$  and  $\text{LaO}^+$  cations reveal that the  $\text{CO}_2$  conversion from the solvated structure into carbonate one is observed for  $[\text{ScO}(\text{CO}_2)_n]^+$  at  $n=5$ , while the  $\text{CO}_2$  molecule is only weakly bound to the metal in  $[\text{LaO}(\text{CO}_2)_n]^+$ . Together with the recent study of the reaction of  $\text{CO}_2$  with  $\text{YO}^+$  [41], it can be found that the  $\text{CO}_2$  fixation into carbonate is accessible by both  $\text{ScO}^+$  and  $\text{YO}^+$  rather than  $\text{LaO}^+$ . Theoretical analyses show that the  $[\text{YO}(\text{CO}_2)_n]^+$  complex has the smallest barrier for the conversion from solvated structure into carbonate one, while  $[\text{LaO}(\text{CO}_2)_n]^+$  exhibits the largest conversion barrier among the three metal oxide cations. The present system affords a model in clarifying how the coordination induces  $\text{CO}_2$  fixation into carbonate by dif-

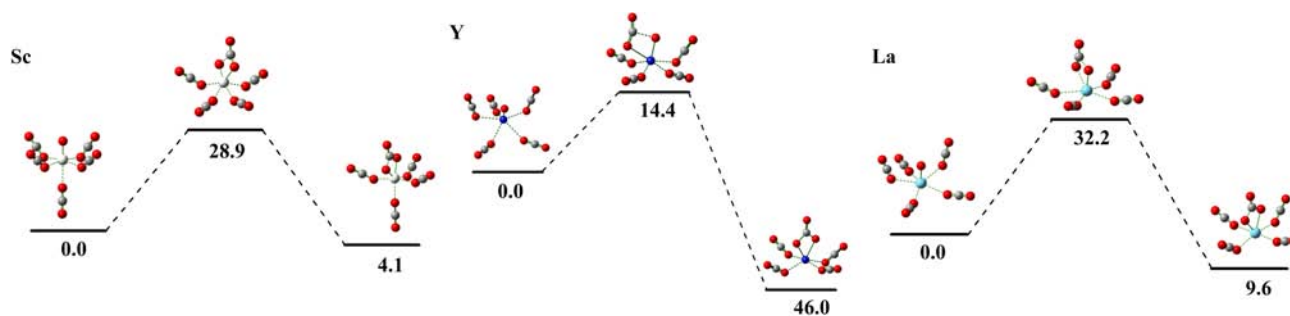


FIG. 5 Potential energy profiles of conversion barrier from solvated structure into carbonate one of  $[\text{MO}(\text{CO}_2)_5]^+$  ( $\text{M}=\text{Sc}$ ,  $\text{Y}$ ,  $\text{La}$ ) calculated at the B2PLYP/def2-TZVP level. Energies are given in kJ/mol.

ferent metal oxides, which should have important implications for the single-atom or single-cluster catalytic transformation of carbon dioxide.

**Supplementary materials:** Mass spectra of  $[\text{ScO}(\text{CO}_2)_n]^+$  and  $[\text{LaO}(\text{CO}_2)_n]^+$  (FIGs. S1 and S2), calculated IR spectra of the solvated and carbonate isomers for  $[\text{LaO}(\text{CO}_2)_n]^+$  (FIG. S3), the Mulliken charges of metal and O atoms of the MO unit in the  $[\text{MO}(\text{CO}_2)_n]^+$  solvated structures (Table S1) are available.

## VI. ACKNOWLEDGMENTS

This work was supported by the National Natural Science Foundation of China (No.21327901, No.21673231, No.21673234, and No.21688102), the Strategic Priority Research Program of Chinese Academy of Sciences (No.XDB17000000), and K. C. Wong Education Foundation.

- [1] T. Sakakura, J. C. Choi, and H. Yasuda, *Chem. Rev.* **107**, 2365 (2007).
- [2] W. Taifan, J. F. Boily, and J. Baltrusaitis, *Surf. Sci. Rep.* **71**, 595 (2016).
- [3] K. Soltys-Brzostek, M. Terlecki, K. Sokolowski, and J. Lewinski, *Coord. Chem. Rev.* **334**, 199 (2017).
- [4] M. North, R. Pasquale, and C. Young, *Green Chem.* **12**, 1514 (2010).
- [5] X. B. Lu and D. J. Darensbourg, *Chem. Soc. Rev.* **41**, 1462 (2012).
- [6] J. Mascetti, F. Galan, and I. Papai, *Coord. Chem. Rev.* **190**, 557 (1999).
- [7] N. R. Walker, R. S. Walters, and M. A. Duncan, *New J. Chem.* **29**, 1495 (2005).
- [8] J. M. Weber, *Int. Rev. Phys. Chem.* **33**, 489 (2014).
- [9] H. Schwarz, *Coord. Chem. Rev.* **334**, 112 (2017).
- [10] L. G. Dodson, M. C. Thompson, and J. M. Weber, *Annu. Rev. Phys. Chem.* **69**, 231 (2018).
- [11] L. Jiang, X. B. Zhang, S. Han, and Q. Xu, *Inorg. Chem.* **47**, 4826 (2008).
- [12] M. F. Zhou and L. Andrews, *J. Am. Chem. Soc.* **120**, 13230 (1998).
- [13] N. R. Walker, G. A. Grieves, R. S. Walters, and M. A. Duncan, *Chem. Phys. Lett.* **380**, 230 (2003).
- [14] G. Gregoire, N. R. Brinkmann, D. van Heijnsbergen, H. F. Schaefer and M. A. Duncan, *J. Phys. Chem. A* **107**, 218 (2003).
- [15] R. S. Walters, N. R. Brinkmann, H. F. Schaefer, and M. A. Duncan, *J. Phys. Chem. A* **107**, 7396 (2003).
- [16] N. R. Walker, R. S. Walters, G. A. Grieves, and M. A. Duncan, *J. Chem. Phys.* **121**, 10498 (2004).
- [17] J. B. Jaeger, T. D. Jaeger, N. R. Brinkmann, H. F. Schaefer, and M. A. Duncan, *Can. J. Chem.* **82**, 934 (2004).
- [18] N. R. Walker, R. S. Walters, and M. A. Duncan, *J. Chem. Phys.* **120**, 10037 (2004).
- [19] G. K. Koyanagi and D. K. Bohme, *J. Phys. Chem. A* **110**, 1232 (2006).
- [20] A. M. Ricks, A. D. Brathwaite, and M. A. Duncan, *J. Phys. Chem. A* **117**, 11490 (2013).
- [21] X. P. Xing, G. J. Wang, C. X. Wang, and M. F. Zhou, *Chin. J. Chem. Phys.* **26**, 687 (2013).
- [22] A. Iskra, A. S. Gentleman, A. Kartouzian, M. J. Kent, A. P. Sharp, and S. R. Mackenzie, *J. Phys. Chem. A* **121**, 133 (2017).
- [23] Z. Zhao, X. Kong, D. Yang, Q. Yuan, H. Xie, H. Fan, J. Zhao, and L. Jiang, *J. Phys. Chem. A* **121**, 3220 (2017).
- [24] D. Yang, X. Kong, H. Zheng, M. Su, Z. Zhao, H. Xie, H. Fan, W. Zhang, and L. Jiang, *J. Phys. Chem. A* **123**, 3703 (2019).
- [25] B. J. Knurr and J. M. Weber, *J. Am. Chem. Soc.* **134**, 18804 (2012).
- [26] B. J. Knurr and J. M. Weber, *J. Phys. Chem. A* **117**, 10764 (2013).
- [27] B. J. Knurr and J. M. Weber, *J. Phys. Chem. A* **118**, 4056 (2014).
- [28] B. J. Knurr and J. M. Weber, *J. Phys. Chem. A* **118**, 10246 (2014).
- [29] B. J. Knurr and J. M. Weber, *J. Phys. Chem. A* **118**, 8753 (2014).
- [30] M. C. Thompson, J. Ramsay, and J. M. Weber, *Angew. Chem. Int. Ed.* **55**, 15171 (2016).
- [31] M. C. Thompson, J. Ramsay, and J. M. Weber, *J. Phys. Chem. A* **121**, 7534 (2017).
- [32] M. C. Thompson and J. M. Weber, *J. Phys. Chem. A* **122**, 3772 (2018).
- [33] A. E. Green, J. Justen, W. Schoellkopf, A. S. Gentle-

- man, A. Fielicke, and S. R. Mackenzie, *Angew. Chem. Int. Ed.* **57**, 14822 (2018).
- [34] L. G. Dodson, M. C. Thompson, and J. M. Weber, *J. Phys. Chem. A* **122**, 29831 (2018).
- [35] L. G. Dodson, M. C. Thompson, and J. M. Weber, *J. Phys. Chem. A* **122**, 6909 (2018).
- [36] F. S. Menges, S. M. Craig, N. Toetsch, A. Bloomfield, S. Ghosh, H. J. Krueger, and M. A. Johnson, *Angew. Chem. Int. Ed.* **55**, 1282 (2016).
- [37] G. B. S. Miller, T. K. Esser, H. Knorke, S. Gewinner, W. Schoellkopf, N. Heine, K. R. Asmis, and E. Uggerud, *Angew. Chem. Int. Ed.* **53**, 14407 (2014).
- [38] H. J. Freund and M. W. Roberts, *Surf. Sci. Rep.* **25**, 225 (1996).
- [39] M. Firouzbakht, M. Schlangen, M. Kaupp, and H. Schwarz, *J. Catal.* **343**, 68 (2016).
- [40] M. R. Sievers and P. B. Armentrout, *Inorg. Chem.* **38**, 397 (1999).
- [41] Z. Zhao, X. Kong, Q. Yuan, H. Xie, D. Yang, J. Zhao, H. Fan, and L. Jiang, *Phys. Chem. Chem. Phys.* **20**, 19314 (2018).
- [42] A. Iskra, A. S. Gentleman, E. M. Cunningham, and S. R. Mackenzie, *Int. J. Mass spectrom.* **435**, 93 (2019).
- [43] Q. Zhang, H. Qu, M. Chen, and M. Zhou, *J. Phys. Chem. A* **120**, 425 (2016).
- [44] H. Xie, J. Wang, Z. B. Qin, L. Shi, Z. C. Tang, and X. P. Xing, *J. Phys. Chem. A* **118**, 9380 (2014).
- [45] M. J. Frisch, G. W. Trucks, H. B. Schlegel, G. E. Scuseria, M. A. Robb, J. R. Cheeseman, G. Scalmani, V. Barone, B. Mennucci, G. A. Petersson, H. Nakatsuji, M. Caricato, X. Li, H. P. Hratchian, A. F. Izmaylov, J. Bloino, G. Zheng, J. L. Sonnenberg, M. Hada, M. Ehara, K. Toyota, R. Fukuda, J. Hasegawa, M. Ishida, T. Nakajima, Y. Honda, O. Kitao, H. Nakai, T. Vreven, J. A. Montgomery Jr., J. E. Peralta, F. Ogliaro, M. J. Bearpark, J. Heyd, E. N. Brothers, K. N. Kudin, V. N. Staroverov, R. Kobayashi, J. Normand, K. Raghavachari, A. P. Rendell, J. C. Burant, S. S. Iyengar, J. Tomasi, M. Cossi, N. Rega, N. J. Millam, M. Klene, J. E. Knox, J. B. Cross, V. Bakken, C. Adamo, J. Jaramillo, R. Gomperts, R. E. Stratmann, O. Yazyev, A. J. Austin, R. Cammi, C. Pomelli, J. W. Ochterski, R. L. Martin, K. Morokuma, V. G. Zakrzewski, G. A. Voth, P. Salvador, J. J. Dannenberg, S. Dapprich, A. D. Daniels, O. Farkas, J. B. Foresman, J. V. Ortiz, J. Cioslowski, and D. J. Fox, *Gaussian 09, Revision A02*, Wallingford, CT: Gaussian, Inc., (2009).
- [46] G. E. Douberly, R. E. Miller, and S. S. Xantheas, *J. Am. Chem. Soc.* **139**, 4152 (2017).
- [47] D. J. Goebbert, T. Wende, L. Jiang, G. Meijer, A. Sanov, and K. R. Asmis, *J. Phys. Chem. Lett.* **1**, 2465 (2010).